

## Internally pumped subthreshold OPO

J.L. Sørensen, E.S. Polzik

Institute of Physics and Astronomy, University of Aarhus, DK-8000 Aarhus C., Denmark  
 (Fax: +45/86120740, E-mail: jls@dfi.aau.dk, polzik@dfi.aau.dk)

Received: 25 February 1998/Revised version: 27 March 1998

**Abstract.** The quantum noise of the internally pumped ring optical parametric oscillator is analyzed theoretically. The fundamental field and subharmonics are assumed to be resonator modes, whereas the second harmonic can have an arbitrary detuning. The threshold for parametric oscillations in this system is derived in a plane-wave approximation. The noise spectra for the fundamental and subharmonics below the threshold are calculated via a semiclassical approach. It is demonstrated that the fundamental beam reflected from this OPO can be perfectly amplitude squeezed around multiples of the free spectrum range frequency. Such a cavity is proposed for use as a quantum amplitude ‘noise eater’.

**PACS:** 42.50Dv, 42.50Lv, 42.65Yj

During recent years, substantial effort has been made to produce squeezed and other nonclassical states of the radiation field via intracavity  $\chi^{(2)}$  nonlinear processes [1, 2]. Applications span from noiseless communications and interferometry [3–6] to atomic physics and spectroscopy [7–10].

Unfortunately the popular scheme of generation of squeezed states via second-harmonic generation and subsequent optical parametric downconversion requires a rather extensive optical setup. These issues motivate the search for a more compact and easily operated source of squeezed light. Towards this goal we consider here the system shown in Fig. 1.

A ring nonlinear resonator with a  $\chi^{(2)}$  crystal is illuminated with the fundamental pump at the frequency  $\omega$ . The second harmonic at  $2\omega$  is generated. The light at  $2\omega$  can now interact with the nonlinear medium either degenerately, producing a field around the fundamental frequency, or nondegenerately, producing subharmonics at frequencies  $\omega_+$  and  $\omega_-$  so that  $\omega = \frac{1}{2}(\omega_+ + \omega_-)$ . This is of course nothing but second-harmonic generation (SHG), where the second harmonic (SH) is pumping a nondegenerate optical parametric oscillator (OPO). We will therefore henceforth refer to this system as the internally pumped OPO (IOPO) as opposed to the externally pumped OPO, where the pump at frequency

$2\omega$  is generated in an external resonator and then injected into the OPO.

The threshold of the internally pumped OPO can be identified as the point where the subharmonic fields start to acquire a coherent amplitude. In this paper we concentrate on the below-threshold IOPO since we know that the externally pumped subthreshold OPO can work as a very efficient source of squeezed vacuum [11, 12].

The cascaded  $\chi^{(2)}$  process above threshold has been treated in [13–15] with all four modes at frequencies  $\omega$ ,  $2\omega$ ,  $\omega_{\pm}$  considered exactly resonant. This device has been demonstrated experimentally in [16, 17], where its classical properties are analyzed. Detailed classical analysis in the case of nonresonant SH is performed in [18] along with the discussion of the twin-beam-like nonclassical correlations between the signal and idler modes analogous to the normal nondegenerate OPO.

In this paper we concentrate on the following attractive feature of the subthreshold system shown in Fig. 1. We note that the light reflected off the input coupler contains both the coherent component at frequency  $\omega$  and the vacuum quantum fields around frequencies  $\omega$  and  $\omega_{\pm}$ . Under ideal experimental conditions the four fields are spatially mode-matched and have well-defined phase relations. As a result one can expect interesting quantum features to occur in the quantum noise of the fundamental pump reflected off the cavity around zero frequency and around frequencies of one free spectrum range (FSR) and its multiples. Therefore, under appropriate conditions, such a cavity alone can serve as a source of amplitude- or phase-squeezed light, eliminating the need for complicated two-cavity setups with external local oscillators. The phase of the squeezed vacuum formed by the intracavity fields  $\omega$  and  $\omega_{\pm}$  with regard to the coherent pump reflected off the cavity depends on the phase of the second-harmonic field. This phase can be changed by detuning the cavity away from the SH resonance, thereby converting the amplitude squeezing into phase squeezing in the field reflected off the cavity. That is why the SH field detuning is considered in such great detail below.

Whereas the quantum noise of the fundamental light reflected off the nonlinear cavity around zero frequency has

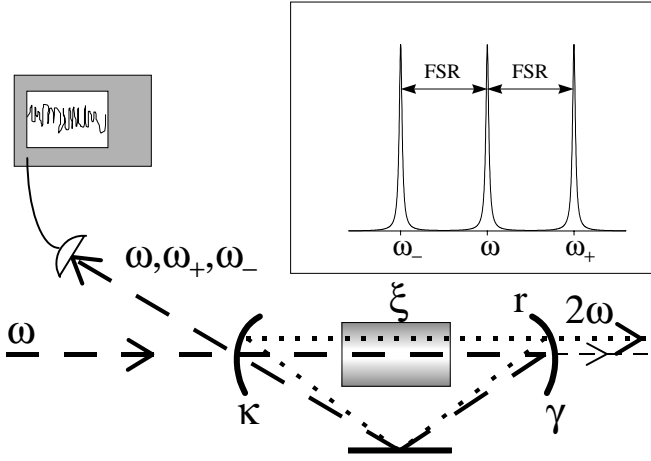


**Fig. 1.** The system under consideration. Dashed lines illustrate the lower frequencies  $\omega$  and  $\omega_{\pm}$  and dotted lines illustrate the second harmonic  $2\omega$ . Insert: the experimental situation in which quantum noise reduction is expected: the fundamental cavity mode ( $\omega$ ) and one free spectrum range (FSR) above and below the frequency of this mode at  $\omega_{+}$  and  $\omega_{-}$ .

been experimentally investigated before [19], the frequency domain around the multiples of the FSR has not been explored. It is in this domain, in fact, where our results look most promising.

The quantum noise of the second harmonic that is generated in a nonlinear cavity has been experimentally investigated by several groups [20–24] and is not treated in this paper.

## 1 Equations of motion

In the following, we will treat the three modes at  $\omega$  and  $\omega_{\pm}$  as resonant cavity modes with no detuning, whereas the fourth mode ( $2\omega$ ) can have arbitrary detuning that is either resonant or nonresonant. It has been shown that it is possible to extract a single cavity mode from the continuum, making a bridge between nonresonant and resonant quantum fields [25]. It should be mentioned that our treatment is not valid in the limit where the losses of the IR modes become comparable to the losses of the second harmonic, since we adiabatically eliminate the SH mode from our equations of motion. Since we want to treat the SH mode  $b$  in both the resonant and the nonresonant case, we have to take the spatial variation of this mode into account. Assuming the modes to be plane waves and ignoring any longitudinal spatial variation of the low-loss cavity modes  $\omega$ ,  $\omega_{\pm}$ , we write the slowly varying SH field envelope inside the nonlinear medium as

$$b(z) = b(0) + i \frac{z}{l} (\xi_1 a_1^2 + \xi_2 a_+ a_-), \quad (1)$$

where  $b(0)$  is the SH field just before the  $\chi^{(2)}$  medium.  $a_1$  is the fundamental mode,  $a_{\pm}$  are the down-converted modes,  $\xi_1$  and  $\xi_2$  are the degenerate and nondegenerate nonlinear coupling constants, respectively, and  $l$  is the length of the nonlinear medium. Close to degeneracy,  $\xi_1$  and  $\xi_2$  are related by  $\xi_2 \simeq 2\xi_1$  and in the rest of this paper we will put  $\xi_2 = 2\xi_1 \equiv 2\xi$ . Integrating (1) we find the SH field immedi-

ately after the nonlinear medium  $b(l)$  to be

$$b(l) = b(0) + i\xi (a_1^2 + 2a_+ a_-). \quad (2)$$

Finally we find  $b(0)$  as the feedback of  $b(l)$  plus a contribution from the vacuum noise entering through the input/output port:

$$b(0) = b(l) r e^{i\delta} + \sqrt{1-r^2} e^{i\delta} \sqrt{\tau} b^{\text{in}}. \quad (3)$$

Here  $\delta$  is the single-round-trip phase shift,  $\tau$  is the cavity round-trip time,  $r$  is the coupler reflectivity and the ‘in’ field is assumed to be in the vacuum state. Solving (2) and (3) for  $b(l)$  and  $b(0)$  we find

$$\begin{aligned} b(0) &= i \frac{r e^{i\delta}}{1 - r e^{i\delta}} \xi (a_1^2 + 2a_+ a_-) + \frac{\sqrt{1-r^2} e^{i\delta}}{1 - r e^{i\delta}} \sqrt{\tau} b^{\text{in}}, \\ b(l) &= \frac{i}{1 - r e^{i\delta}} \xi (a_1^2 + 2a_+ a_-) + \frac{\sqrt{1-r^2} e^{i\delta}}{1 - r e^{i\delta}} \sqrt{\tau} b^{\text{in}}. \end{aligned} \quad (4)$$

For the remaining cavity modes we can now readily provide the round-trip increments:

$$\begin{aligned} \Delta a_1 &= \left[ \sqrt{2\kappa} \mathcal{E} - (\kappa + \gamma) a_1 \right] \tau + 2i\xi \int_0^1 d\left(\frac{z}{l}\right) a_1^\dagger b(z) \\ &\quad + \tau \sqrt{2\kappa} a_1^{\text{in}} + \tau \sqrt{2\gamma} \alpha_1^{\text{in}}, \\ \Delta a_{\pm} &= -(\kappa + \gamma) \tau a_{\pm} + 2i\xi \int_0^1 d\left(\frac{z}{l}\right) a_{\mp}^\dagger b(z) \\ &\quad + \tau \sqrt{2\kappa} a_{\pm}^{\text{in}} + \tau \sqrt{2\gamma} \alpha_{\pm}^{\text{in}}. \end{aligned} \quad (5)$$

Here  $\kappa$  is the fundamental decay rate through the coupler,  $\gamma$  represents all other losses of the fundamental,  $\mathcal{E}$  is the c-number pump field at the fundamental frequency and the ‘in’ fields are vacuum fields as usual. We have assumed all low-frequency decay rates to be equal,  $\kappa_+ = \kappa_- = \kappa$  and  $\gamma_+ = \gamma_- = \gamma$ , which is justified by the fact that we are mostly interested in three adjacent longitudinal modes of the cavity. Using (1) and (4) we can evaluate the above integrals to obtain the basic equations of motion governing the system:

$$\begin{aligned} \frac{da_1}{dt} &= \sqrt{2\kappa} \mathcal{E} - (\kappa + \gamma) a_1 - \frac{\xi^2}{\tau} g a_1^\dagger (a_1^2 + 2a_+ a_-) \\ &\quad + \sqrt{2\kappa} a_1^{\text{in}} + \sqrt{2\gamma} \alpha_1^{\text{in}} + 2 \frac{\xi}{\sqrt{\tau}} j a_1^\dagger b^{\text{in}}, \\ \frac{da_{\pm}}{dt} &= -(\kappa + \gamma) a_{\pm} - \frac{\xi^2}{\tau} g a_{\mp}^\dagger (a_1^2 + 2a_+ a_-) \\ &\quad + \sqrt{2\kappa} a_{\pm}^{\text{in}} + \sqrt{2\gamma} \alpha_{\pm}^{\text{in}} + 2 \frac{\xi}{\sqrt{\tau}} j a_{\mp}^\dagger b^{\text{in}}, \\ b(l) &= h \xi (a_1^2 + 2a_+ a_-) - i \sqrt{\tau} j b^{\text{in}}. \end{aligned} \quad (6)$$

The resonance properties of the SH field are contained in the functions  $g$ ,  $j$ , and  $h$ , defined as

$$\begin{aligned} g &= (1 + r e^{i\delta}) (1 - r e^{i\delta})^{-1} \equiv g_R (1 + iQ), \\ h &= i (1 - r e^{i\delta})^{-1} \equiv h_R (1 + iR), \\ j &= i \left( \sqrt{1 - r^2} e^{i\delta} \right) (1 - r e^{i\delta})^{-1} \equiv j_R (1 + i\Sigma), \end{aligned} \quad (7)$$

with  $\varrho$  given by

$$\varrho = -\frac{2r \sin \delta}{1-r^2}. \quad (8)$$

In the limit of nonresonant SH ( $g = 1$ ) the equations of motion (6) are equivalent to the Langevin equations derived by adiabatic elimination the SH field from a nonlinear Hamiltonian of the form

$$H = \hbar \left[ \chi_1 \left( a_1^\dagger a_1^2 + (a_1^\dagger)^2 a_2 \right) + \chi_2 \left( a_1^\dagger a_1^\dagger a_2 + a_2^\dagger a_+ a_- \right) \right]. \quad (9)$$

Because of this we do not expect our treatment to be valid in the limit where SH and IR losses are comparable, since adiabaticity will break down then.

We now introduce the quadrature phases  $X_1, Y_1, X_2, Y_2, X_+, Y_+, X_-,$  and  $Y_-$ , defined as

$$\begin{aligned} X_1 &= a_1 e^{i\theta_1} + a_1^\dagger e^{-i\theta_1}, Y_1 = -i \left( a_1 e^{i\theta_1} - a_1^\dagger e^{-i\theta_1} \right), \\ X_2 &= b e^{i\theta_2} + b^\dagger e^{-i\theta_2}, Y_2 = -i \left( b e^{i\theta_2} - b^\dagger e^{-i\theta_2} \right), \end{aligned} \quad (10)$$

and

$$\begin{aligned} X_\pm &= \frac{1}{\sqrt{2}} \left[ (a_+ \pm a_-) e^{i\phi} + (a_+^\dagger \pm a_-^\dagger) e^{-i\phi} \right], \\ Y_\pm &= \frac{-i}{\sqrt{2}} \left[ (a_+ \pm a_-) e^{i\phi} - (a_+^\dagger \pm a_-^\dagger) e^{-i\phi} \right], \end{aligned} \quad (11)$$

where our phases  $\theta_1, \theta_2,$  and  $\phi$  are defined relative to the pump phase, which we set to zero, meaning that we can choose  $\mathcal{E} = \mathcal{E}^*$ . We can use (6) together with their Hermitian conjugates to obtain the equations of motion for the quadratures. Unfortunately these are rather lengthy and will therefore not be reproduced here, but, as shown below, the equations are considerably simplified by choosing the phases  $\theta_1, \theta_2,$  and  $\phi$  appropriately.

## 2 Steady-state solutions

With the goal of determining the threshold of the OPO and the steady-state values of the fields, we solve below the classical equations of motion. These are obtained by taking the expectation values of the field operators in the equations of motion derived in the previous section. The ‘in’ fields are in the vacuum state, meaning that they will not contribute to the solutions.

Ignoring for now the trivial solution of all subharmonics being in the vacuum state, we focus on the threshold of the IOPO. Looking for steady-state solutions above the OPO threshold, we choose the steady-state fields such that  $\bar{Y}_1 = \bar{X}_- = \bar{Y}_+ = 0$ . This requires a certain choice of the quadrature phases so that the real axis is chosen along the coherent amplitudes of the fields. Now our equations of motion for the subharmonics simplify to

$$\left[ Z^2 + \left( \frac{\kappa + \gamma}{A} \right)^2 \right]^2 + \varrho^2 Z^4 = (1 + \varrho^2) \bar{X}_1^4. \quad (12)$$

Here we have defined  $A = \xi^2 g_R / 4\tau$  and  $Z^2 = \bar{X}_+^2 + \bar{Y}_-^2$ . The solution of (12) becomes real for the intracavity fundamental field of

$$X_1^{\text{th}} = \sqrt{\frac{\kappa + \gamma}{A\sqrt{1 + \varrho^2}}} = \frac{2}{\xi} \sqrt{\frac{(\kappa + \gamma)\tau}{|g|}}. \quad (13)$$

This is obviously the value of the intracavity fundamental field required to drive the IOPO above threshold. Now we can readily write the subharmonic excitation as

$$Z^2 = \frac{(X_1^{\text{th}})^2}{\sqrt{1 + \varrho^2}} \left[ \sqrt{\left( \left[ \bar{X}_1 / X_1^{\text{th}} \right]^4 - 1 \right) (1 + \varrho^2) + 1} - 1 \right]. \quad (14)$$

For zero SH detuning this reduces to the well-known result [27–29]

$$Z = X_1^{\text{th}} \sqrt{\left[ \bar{X}_1 / X_1^{\text{th}} \right]^2 - 1} \quad (15)$$

found for the externally pumped OPO. Only our subharmonic is expressed in terms of the fundamental pump, whereas the pump for a standard OPO is usually described by the SH field strength. Using the symmetry of the problem, we can now deduce the steady-state subharmonic quadratures above threshold to be  $\bar{X}_+ = \bar{Y}_- = Z / \sqrt{2}$ .

Similarly we find the equation of motion for the fundamental below threshold:

$$\bar{X}_1 \left( \bar{X}_1^2 + \frac{\kappa + \gamma}{A} \right) = \frac{\sqrt{8\kappa\mathcal{E}}}{A} \cos \theta_1, \quad (16)$$

where the phase of the fundamental is given by

$$\sin \theta_1 = \frac{\varrho A}{\sqrt{8\kappa\mathcal{E}}} \bar{X}_1^3. \quad (17)$$

By inserting (13) and (17) into (16), we find the external field strength required to drive the OPO above threshold to be

$$\mathcal{E}_{\text{th}} = X_1^{\text{th}} \frac{\kappa + \gamma}{2\sqrt{\kappa}} \sqrt{1 + \frac{1}{\sqrt{1 + \varrho^2}}}. \quad (18)$$

The corresponding threshold power for the IOPO can now be derived to be

$$P_{\text{th}} = \frac{(\mathcal{T} + \mathcal{L})^3}{2\mathcal{T} E_{\text{NL}}} \frac{1}{|g|} \left( 1 + \frac{1}{\sqrt{1 + \varrho^2}} \right), \quad (19)$$

where the single-pass nonlinearity for second-harmonic generation,  $E_{\text{NL}} = P(2\omega) / P^2(\omega)$ , can be found from (2) by setting the down-converted fields to zero.  $\mathcal{T}$  and  $\mathcal{L}$  are the cavity coupler transmission and the residual intracavity losses for the fundamental field. In the limit  $\varrho \rightarrow 0$  the functional dependence of the obtained threshold on the cavity parameters is similar to that obtained in [18]. To minimize this threshold we should choose the coupler transmission to be equal to half the losses. This, however, is not the optimum choice when one wants to maximize the squeezing in the IOPO output. As shown below, the degree of observable squeezing is

limited by, among other things, the OPO escape efficiency  $\mathcal{T}/(\mathcal{T} + \mathcal{L})$ . From this it is clear that when the threshold is minimized at  $\mathcal{T} = \frac{1}{2}\mathcal{L}$ , the escape efficiency allows for maximum 33% quantum noise reduction. In order to maximize squeezing, one should minimize the losses  $\mathcal{L}$  and have  $\mathcal{T}$  as large as possible compatible with the available pumping power. The effect of the SH feedback on the threshold is mainly hidden in the function  $|g|$ , from which it is clear that the threshold can be drastically reduced if  $r \lesssim 1$  and  $\delta = 0$  corresponding to a high build up of the second harmonic. If, however,  $\delta \simeq \pi$ , the threshold becomes very high because of destructive interference of the fed-back second harmonic.

Choosing  $\mathcal{L} = 0.5\%$ ,  $E_{\text{NL}} = 0.02 \text{ W}^{-1}$ , as for a good KNbO<sub>3</sub> crystal [11], taking  $\mathcal{T} = 5\%$  and furthermore assuming nonresonant SH ( $r = 0$ ) so that  $\varrho = 0$  and  $|g| = 1$ , we find a threshold of  $P_{\text{th}} \simeq 170 \text{ mW}$ , which is well within reach of modern coherent light sources. In fact a threshold of 120 mW has been observed in experimentally in [17]. It should be stressed at this point that our treatment is only valid in the plane-wave approximation. The IOPO threshold calculations for focused Gaussian beams give results that typically do not differ by more than a factor of two [26]. The threshold calculations for focussed Gaussian beams can be also found in [18].

In operation below the OPO threshold the down-converted fields are all zero and, furthermore, we can put  $\bar{Y}_1 = 0$  if the fundamental quadrature phase is chosen according to (17). The fundamental field is now found as the solution of (16) by using the definition (17).  $\bar{X}_1$ , per definition, is real, so the solution can readily be picked to be

$$\bar{X}_1 = X_1^{\text{th}} \Gamma(\sigma, \varrho), \quad \sigma < 1, \quad (20)$$

where  $\Gamma(\sigma, \varrho) = \sqrt{z(\sigma, \varrho)}$ , and  $z(\sigma, \varrho)$  is given as the real solution of

$$\sqrt{1 + \varrho^2} z(1 + z^2) + 2z^2 - 2\sigma^2 (1 + \sqrt{1 + \varrho^2}) = 0. \quad (21)$$

Here we have defined the pump parameter  $\sigma = \mathcal{E}/\mathcal{E}_{\text{th}} = \sqrt{P/P_{\text{th}}}$ . It can be checked that in the limit of a perfectly resonant second harmonic ( $\varrho = 0$ ) this solution reduces to what is found in doubly resonant SHG with the replacement of  $\mathcal{E}_{\text{th}}$  with the critical pump field required to reach the point of self-oscillations. From Fig. 2 we see that  $\Gamma$  grows from 0 with no pump to 1 as the OPO approaches threshold.

Substituting the solution (20) into (17) we obtain the natural choice of the fundamental quadrature phase:

$$\theta_1 = \arcsin \left( \frac{\varrho \Gamma^3}{\sigma \sqrt{2\sqrt{1 + \varrho^2} (1 + \sqrt{1 + \varrho^2})}} \right). \quad (22)$$

By choosing the second-harmonic quadrature phase as

$$\theta_2 = 2\theta_1 + \arctan R^{-1}, \quad (23)$$

we find the stationary values for this field below threshold to be

$$\begin{aligned} \bar{X}_2(l) &= 0, \\ \bar{Y}_2(l) &= Y_2^{\text{th}} \Gamma^2(\sigma, \varrho), \quad \sigma < 1, \end{aligned} \quad (24)$$

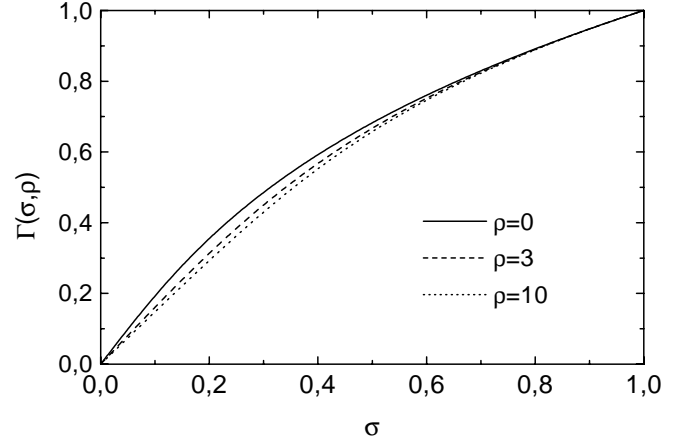


Fig. 2. The steady-state fundamental build up  $\Gamma(\sigma, \rho) = \bar{X}_1/X_1^{\text{th}}$  as a function of the pump parameter  $\sigma$

where we have defined the threshold intracavity SH field as  $Y_2^{\text{th}} = \frac{1}{2}\xi |h| (X_1^{\text{th}})^2$ . Again this is similar to the doubly resonant SHG result with the above-mentioned substitution.

### 3 Quantum noise

With the steady-state fields at hand we can now linearize the fluctuations around these operating points by using a Langevin approach usually referred to as the semiclassical approach [30]. Consequently we do not expect our results to be valid in a situation with strong nonlinear interaction, which is the case very close to the OPO threshold. In this regime, higher-order corrections come into play; more rigorous treatments can be found in [31–33]. In this paper we limit ourselves to the IOPO below threshold since it is known from standard OPO theory that this is where the best quadrature phase squeezing is generated [27, 28]. Furthermore, the quantum noise of the second harmonic will not be calculated in this paper since it has been shown that more elaborate methods are required to deal with the quasi-resonant behavior of this field [34].

Defining the fluctuation operators  $q_i$  and  $p_i$  as

$$q_i = X_i - \bar{X}, \quad p_i = Y_i - \bar{Y}_i, \quad i = 1, +, -, \quad (25)$$

we insert (25) together with the  $\sigma < 1$  steady-state values in our equations of motion. Assuming small fluctuations, we keep terms up to the first order to obtain the equations of motion for the fluctuations of the fundamental,

$$\begin{aligned} \frac{d}{d(\kappa + \gamma)t} \begin{pmatrix} q_1 \\ p_1 \end{pmatrix} &= - \left[ \mathbb{I} + \Gamma^2 \begin{pmatrix} 3 & -\varrho \\ 3\varrho & 1 \end{pmatrix} \right] \begin{pmatrix} q_1 \\ p_1 \end{pmatrix} \\ &+ \frac{\sqrt{2\kappa}}{\kappa + \gamma} \begin{pmatrix} q_1^{\text{in}} \\ p_1^{\text{in}} \end{pmatrix} + \frac{\sqrt{2\gamma}}{\kappa + \gamma} \begin{pmatrix} Q_1^{\text{in}} \\ P_1^{\text{in}} \end{pmatrix} \\ &+ \frac{2\Gamma}{\sqrt{(\kappa + \gamma)}} \begin{pmatrix} q_2^{\text{in}} \\ p_2^{\text{in}} \end{pmatrix}, \end{aligned} \quad (26)$$

and for the subharmonics,

$$\begin{aligned} \frac{d}{d(\kappa + \gamma)t} \begin{pmatrix} q_{\pm} \\ p_{\pm} \end{pmatrix} = & - \left[ \mathbb{I} \pm \Gamma^2 \sqrt{1 + \varrho^2} \mathbb{S} \right] \begin{pmatrix} q_{\pm} \\ p_{\pm} \end{pmatrix} \\ & + \frac{\sqrt{2\kappa}}{\kappa + \gamma} \begin{pmatrix} q_{\pm}^{\text{in}} \\ p_{\pm}^{\text{in}} \end{pmatrix} \\ & + \frac{\sqrt{2\gamma}}{\kappa + \gamma} \begin{pmatrix} Q_{\pm}^{\text{in}} \\ P_{\pm}^{\text{in}} \end{pmatrix}. \end{aligned} \quad (27)$$

Here  $\mathbb{I}$  is the unit matrix and  $\mathbb{S} = \begin{pmatrix} 1 & 0 \\ 0 & -1 \end{pmatrix}$ . We have also defined the fundamental quadrature phase as (22) and the second-harmonic quadrature phase as  $\theta_2 = \arctan \Sigma + 2\theta_1$ , where  $\Sigma$  is defined in (7), and finally we have chosen the subharmonic quadrature phase to be

$$\phi = \theta_1 - 1/2 \arctan \varrho. \quad (28)$$

All 'in' fields above are assumed to be independent and in the vacuum state. After the Fourier transformation we arrive at

$$\begin{aligned} \left[ (i\bar{\omega} + 1) \mathbb{I} + \Gamma^2 \begin{pmatrix} 3 & -\varrho \\ 3\varrho & 1 \end{pmatrix} \right] \begin{pmatrix} q_1 \\ p_1 \end{pmatrix} = & \frac{\sqrt{2\kappa}}{\kappa + \gamma} \begin{pmatrix} q_1^{\text{in}} \\ p_1^{\text{in}} \end{pmatrix} \\ & + \frac{\sqrt{2\gamma}}{\kappa + \gamma} \begin{pmatrix} Q_1^{\text{in}} \\ P_1^{\text{in}} \end{pmatrix} \\ & + \frac{2\Gamma}{\sqrt{(\kappa + \gamma)}} \begin{pmatrix} q_2^{\text{in}} \\ p_2^{\text{in}} \end{pmatrix} \end{aligned} \quad (29)$$

and

$$\begin{aligned} \left[ (i\bar{\omega} + 1) \mathbb{I} \pm \Gamma^2 \sqrt{1 + \varrho^2} \mathbb{S} \right] \begin{pmatrix} q_{\pm} \\ p_{\pm} \end{pmatrix} = & \frac{\sqrt{2\kappa}}{\kappa + \gamma} \begin{pmatrix} q_{\pm}^{\text{in}} \\ p_{\pm}^{\text{in}} \end{pmatrix} \\ & + \frac{\sqrt{2\gamma}}{\kappa + \gamma} \begin{pmatrix} Q_{\pm}^{\text{in}} \\ P_{\pm}^{\text{in}} \end{pmatrix} \end{aligned} \quad (30)$$

for the fluctuations of the low-loss fields. Here  $\bar{\omega} = \omega/(\kappa + \gamma)$ .

To obtain the IOPO output fields (which is what can be detected) we apply the boundary conditions of a field  $F$  on the output coupler:

$$F^{\text{out}} = \sqrt{2\kappa} F - F^{\text{in}}. \quad (31)$$

Here we assume that the coupler transmission is small relative to 1.

### 3.1 Noise of the fundamental

The output fundamental field quadratures obey the equation

$$\begin{aligned} \begin{pmatrix} q_1^{\text{out}} \\ p_1^{\text{out}} \end{pmatrix} = & (2\eta \mathbb{M}^{-1} - \mathbb{I}) \begin{pmatrix} q_1^{\text{in}} \\ p_1^{\text{in}} \end{pmatrix} \\ & + 2\sqrt{\eta(1-\eta)} \mathbb{M}^{-1} \begin{pmatrix} Q_1^{\text{in}} \\ P_1^{\text{in}} \end{pmatrix} + 2\Gamma \sqrt{2\eta} \mathbb{M}^{-1} \begin{pmatrix} q_2^{\text{in}} \\ p_2^{\text{in}} \end{pmatrix}, \end{aligned} \quad (32)$$

where we have defined

$$\mathbb{M} = \left[ (i\bar{\omega} + 1) \mathbb{I} + \Gamma^2 \begin{pmatrix} 3 & -\varrho \\ 3\varrho & 1 \end{pmatrix} \right] \quad (33)$$

and the OPO escape efficiency  $\eta = \kappa/(\kappa + \gamma) \simeq \mathcal{T}/(\mathcal{T} + \mathcal{L})$ , where the last equality requires  $\mathcal{T}, \mathcal{L} \ll 1$ .

To calculate to spectrum of noise we take into account that the 'in' fields are uncorrelated

$$\begin{aligned} \langle q_i^{\text{in}}(-\omega) q_j^{\text{in}}(\omega) \rangle &= \delta_{ij} = \langle p_i^{\text{in}}(-\omega) p_j^{\text{in}}(\omega) \rangle \\ \langle q_i^{\text{in}}(-\omega) p_j^{\text{in}}(\omega) \rangle &= 0 = \langle p_i^{\text{in}}(-\omega) q_j^{\text{in}}(\omega) \rangle \end{aligned} \quad (34)$$

Here we have normalized the white spectrum of vacuum noise of the input fields in the bandwidth relevant to the measurement. Using these definitions we obtain the following noise spectrum for the fundamental amplitude quadrature:

$$\begin{aligned} \langle (\Delta q_1^{\text{out}})^2 \rangle = & \quad (35) \\ 1 - & \frac{4\eta\Gamma^2 \left[ \bar{\omega}^2 + (1 + \Gamma^2)^2 + \varrho^2\Gamma^2(2 - \Gamma^2) \right]}{\left[ (1 + \Gamma^2)(1 + 3\Gamma^2) + 3\varrho^2\Gamma^4 - \bar{\omega}^2 \right]^2 + 4\bar{\omega}^2(1 + 2\Gamma^2)^2}. \end{aligned}$$

Analogous we find for the phase quadrature

$$\begin{aligned} \langle (\Delta p_1^{\text{out}})^2 \rangle = & \quad (36) \\ 1 + & \frac{4\eta\Gamma^2 \left[ \bar{\omega}^2 + (1 + 3\Gamma^2)^2 + \varrho^2\Gamma^2(2 + 3\Gamma^2) \right]}{\left[ (1 + \Gamma^2)(1 + 3\Gamma^2) + 3\varrho^2\Gamma^4 - \bar{\omega}^2 \right]^2 + 4\bar{\omega}^2(1 + 2\Gamma^2)^2}. \end{aligned}$$

The amplitude quadrature (35) is where the quantum noise reduction occurs. For zero detuning of the SH ( $\varrho = 0$ ) at  $\bar{\omega} = 0$  this variance reduces to

$$\langle (\Delta q_1^{\text{out}})^2 \rangle = 1 - \frac{4\eta\Gamma^2}{(1 + 3\Gamma^2)^2}. \quad (37)$$

This is similar to what is found for the two-photon absorber [35] and for the singly resonant second-harmonic generator [21] when the SH is adiabatically eliminated. The minimum of (37) is found for no internal losses ( $\eta = 1$ ) to be  $2/3$ , corresponding to quantum noise reduction of 1.76 dB below the standard quantum limit. The corresponding value of  $\Gamma$  is  $\Gamma(\sigma, \varrho = 0) = 3^{-1/2}$ , meaning that the pump parameter is  $\sigma = 0.385$ .

More exciting are the results for a finite SH detuning ( $\varrho \neq 0$ ). As  $\varrho$  becomes large, corresponding to almost complete dephasing of the SH, the noise in the amplitude quadrature, now rotated relative to the pump according to (22), goes towards  $1/3$ . This happens around a frequency  $\omega^{\text{opt}}$ , which increases with increasing  $\varrho$  and pump,  $\sigma$ . However, for every value of  $\varrho$  there is a corresponding value of the pump,  $\sigma^{\text{opt}}$ , which minimizes the noise. Numerically it is found that  $\sigma^{\text{opt}}$  decreases as  $\varrho$  increases. The spectra are shown in Fig. 3. From the experimental point of view this region is difficult to access since the threshold of the IOPO becomes very high with this choice of  $\varrho$ . Furthermore in order to detect this particular quadrature, the IOPO cavity must be completely impedance matched to the external pump since any pump reflected off the cavity will have a different phase than the intracavity fundamental. This will result in a phase shift of the net reflected field, meaning that the amplitude noise will be

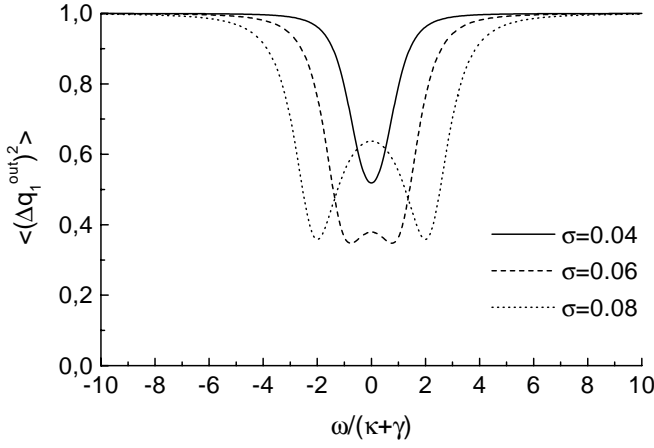


Fig. 3. Noise spectra of the fundamental for the detuning parameter  $\rho = 100$

set by a mixture of the ‘pure’ quadratures defined by  $\theta_1$  in (22).

### 3.2 Noise of the subharmonics

Following the procedure of the preceding section we can readily give the noise spectra for the down-converted fields:

$$\langle (\Delta q_+^{\text{out}})^2 \rangle = \langle (\Delta p_-^{\text{out}})^2 \rangle = 1 - \eta \frac{4\Gamma^2 \sqrt{1+q^2}}{\bar{\omega}^2 + (1 + \Gamma^2 \sqrt{1+q^2})^2}, \quad (38)$$

$$\langle (\Delta p_+^{\text{out}})^2 \rangle = \langle (\Delta q_-^{\text{out}})^2 \rangle = 1 + \eta \frac{4\Gamma^2 \sqrt{1+q^2}}{\bar{\omega}^2 + (1 - \Gamma^2 \sqrt{1+q^2})^2}, \quad (39)$$

where  $\bar{\omega}$  and  $\eta$  are defined as in the previous section. However,  $\bar{\omega} = 0$  now corresponds to the FSR frequency.

For the perfectly resonant SH ( $q = 0$ ) this is not surprisingly the same result as one would get for the externally pumped OPO provided we use the substitution  $\sigma \leftrightarrow \Gamma^2$ . Obviously the substitution is necessary since the threshold for the internally pumped OPO has been derived for the fundamental field, whereas in [27–29] the threshold is derived for the SH pump field. In our case the SH pump field is proportional to the square of the intracavity fundamental field, which has a build-up described by  $\Gamma$ , therefore the substitution is required for comparison.

For zero SH detuning, the noise in the subharmonics is zero at  $\bar{\omega} = 0$  when  $\Gamma^2 = 1 = \eta$ , corresponding to the IOPO being exactly on threshold and having no internal losses. For a finite  $q$ , however, Fig. 4 shows the squeezing reduces in size and the spectrum gets broader because of the dephasing of the second-harmonic pump. In some sense this corresponds to pumping a standard OPO with a field containing lots of phase noise. The noisy pump phase will cause jitter in the phase of the down-converted fields and consequently a mixing of the squeezed and antisqueezed quadratures working to cancel the squeezing.

In order to elaborate a bit more on the spectrum of squeezing (38), let us consider the case where the SH detuning is zero, meaning that  $q = 0$ . Having the amount  $P$  of pump

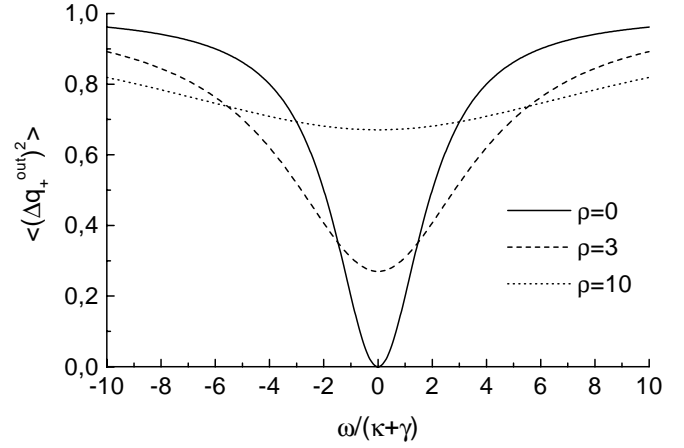


Fig. 4. Squeezing around the nondegenerate frequency on threshold ( $\sigma = 1$ ) and with no internal losses ( $\eta = 1$ ). The squeezing is seen to be perfect for no SH detuning ( $\rho = 0$ ) only to reduce as the SH detuning parameter  $\rho$  is increased

power available, and the fundamental cavity losses of  $\mathcal{T} + \mathcal{L}$ , we can now calculate the pump parameter  $\sigma$ , using (19). This is given by

$$\sigma^2 = PE_{\text{NL}} \frac{\mathcal{T}}{(\mathcal{T} + \mathcal{L})^3} \frac{1+r}{1-r}, \quad (40)$$

where  $r$  is the mirror reflectivity to the SH field. By using (40),  $\Gamma^2(\sigma, q = 0)$  can now be found as the solution to  $z^3 + 2z^2 + z - 4\sigma^2 = 0$ . When  $\sigma$  is less than about 0.6, the solution can, to a good approximation, be written as  $\Gamma^2 = \frac{1}{4} (\sqrt{1 + 32\sigma^2} - 1)$ . If we now insert the found quantities into (38), we obtain the noise power in the squeezed quadratures around the FSR frequency:

$$\langle (\Delta q_+^{\text{out}})^2 \rangle = \langle (\Delta p_-^{\text{out}})^2 \rangle = 1 - \frac{\mathcal{T}}{\mathcal{T} + \mathcal{L}} \frac{\sqrt{1 + 32\sigma^2} - 1}{\bar{\omega}^2 + \left[ 1 + \frac{1}{4} (\sqrt{1 + 32\sigma^2} - 1) \right]^2}, \quad (41)$$

where we assumed the fundamental losses to be small, so that the escape efficiency can be approximated by  $\eta = \mathcal{T}/(\mathcal{T} + \mathcal{L})$ . Knowing the parameters for the nonlinear resonator,  $E_{\text{NL}}$ ,  $\mathcal{T}$ ,  $\mathcal{L}$ ,  $r$ , and the linewidth, it is now straightforward to calculate the predicted squeezing around the FSR frequency by means of (40) and (41).

### 3.3 Noise spectra of the light reflected off the cavity

Having now in mind an experiment where the amplitude noise of the cavity reflection is recorded (Fig. 1), we must consider the interference of the field coming from inside the cavity and the field reflected directly off the cavity. The measurement is assumed to have enough bandwidth, so that the noise of the fundamental as well as the beat note of the down-converted fields against the fundamental carrier can be detected.

The standard beamsplitter relations now give us the following steady-state reflected field:

$$\bar{X}^{\text{ref}} = -2\mathcal{E} + \sqrt{2\kappa} \bar{X}_1 e^{-i\theta_1}. \quad (42)$$

This means that the overall phase  $\psi$  of the reflected field will be given by

$$\psi = -\arctan \left[ \frac{\sin \theta_1}{\cos \theta_1 - \frac{\sigma}{\sqrt{2}\eta\Gamma} \sqrt{1 + \frac{1}{1+\varrho^2}}} \right]. \quad (43)$$

and we can now easily calculate the amplitude noise of the field. This is done by using (22) and (28) to project the noise calculated in the two preceding sections onto the coherent amplitude of the reflected field since this is now serving as a local oscillator for the detection. We plot the spectra of amplitude noise for different detunings in Fig. 5. In this figure the free spectrum range (FSR) of the cavity has been considered to be 50 line widths. For zero detuning of the SH at zero frequency we find 25% noise reduction, but going one FSR away in frequency we find perfect squeezing due to the nondegenerate OPO operation causing perfect field correlation at this frequency. The reason for this is that the OPO has high gain only at cavity resonance, meaning that the interesting effects in the quantum noise occur at zero frequency and at any frequency an integer times the FSR. Of course this is only valid as long as the phase-matching condition is still fulfilled to a reasonable extent. At zero frequency, however, the interaction with the second harmonic has to be taken into account, resulting in only 25% noise reduction at threshold as opposed to perfect squeezing at FSR frequency.

With a finite detuning of the SH, this field dephases, causing degradation of the squeezing according to the discussion in the previous section. In addition to this, the purely squeezed and antisqueezed quadratures will now start mixing, and as a result a noise spike from the strongly anti-squeezed quadrature of the subharmonic enters the spectrum at a frequency of one FSR. This happens even for very small SH detunings,  $\varrho$ , meaning that good control of the SH phase is required in order to observe appreciable squeezing in the subharmonics.

The low-frequency squeezing is smaller and consequently more robust against the phase shift. For the values of  $\varrho$  used in Fig. 5 this squeezing almost does not reduce. Note that whereas maximum amplitude squeezing in the subharmonics (around FSR frequency) can be observed in

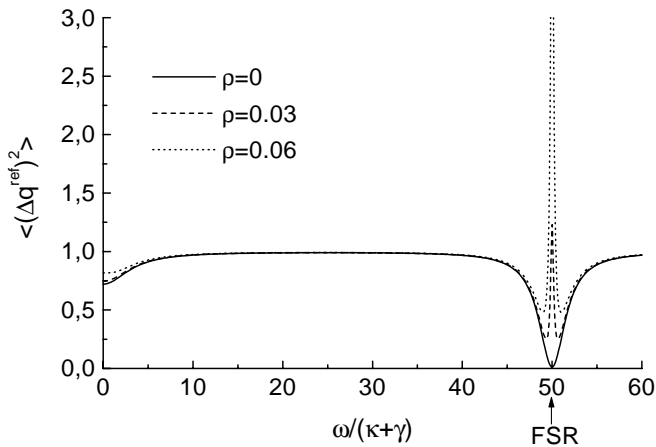


Fig. 5. Spectrum of amplitude noise of the reflection of the IOPO. The traces corresponds to a pump of  $\sigma = 0.8$  and no internal losses  $\eta = 1$

the reflection off the cavity, maximum amplitude squeezing in the fundamental (around zero frequency) requires the use of the LO with the phase different from the phase of the reflected fundamental field (compare Figs. 3, 4, and 5). This fact, along with the greater degree of noise reduction predicted in the subharmonics, leads to the attractiveness that we attach to the observation of the quantum noise in reflection off the IOPO at the FSR frequency.

In more practical terms, the squeezing in the subharmonics with no SH feedback ( $\varrho = 0$ ), close to threshold ( $\sigma \gtrsim 0.8$ ) is seen from (38) to be limited mainly by the escape efficiency  $\eta = \mathcal{T} / (\mathcal{T} + \mathcal{L})$ . By using (19), we find that in order to reach the degree of squeezing equal to  $\eta$ , given that the IOPO has losses  $\mathcal{L}$  and nonlinearity  $E_{\text{NL}}$ , we need the pump power of  $P = \sigma^2 \mathcal{L}^2 / \eta (1 - \eta)^2 E_{\text{NL}}$  from our laser. The corresponding output coupler transmission is given by  $\mathcal{T} = \mathcal{L} \eta / (1 - \eta)$ . If we use realistic parameters of  $\sigma = 0.8$ ,  $\mathcal{L} = 0.005$ ,  $\eta = 0.9$ , and  $E_{\text{NL}} = 0.02 \text{ W}^{-1}$ , we find that  $\mathcal{T} = 0.045$  and that the pump power of  $P = 90 \text{ mW}$  is required. Again we note that these results apply only in a plane-wave approximation (see the discussion above).

Finally we want to emphasize that the results given so far rely on perfect spatial mode matching of the pump wave into the IOPO cavity. Any mismatch will result in a threshold increased with the amount  $\mu^{-1}$ , where  $\mu$  is the degree of mode matching. Worse is the effect on the quantum noise reduction in the reflection of the cavity. Here any mismatch will correspond to mixing  $1 - \mu$  units of vacuum noise into the squeezing, resulting in a noisier reflection.

## 4 Summary

We have treated the internally pumped optical parametric oscillator with the fundamental and down-converted fields resonant and the second harmonic nonresonant or partly resonant with an arbitrary detuning. We derive the threshold of parametric oscillations for this device. It is found to depend critically on the properties of the cavity with respect to the second harmonic. The threshold in principle goes from zero for the perfectly resonant second harmonic to infinity for the perfectly resonant but detuned second harmonic. The details of this behavior are described by the function  $|g|^{-1}$ , defined in (7). The steady-state fields inside the nonlinear resonator are derived below threshold and their amplitudes are shown to be governed by the function  $\Gamma(\sigma, \varrho)$  (20). Our treatment assumes all fields to be plane waves and does not include the problem of phase matching (for details of the effect of finite focusing see [18, 26]).

In general, the issue of feeding back the SH by means of increasing the SH finesse raises questions similar to the case of the regular OPO. Namely, resonant SH allows us to reduce the required pumping power but leads to additional complications with tunability and the need to preserve several simultaneous resonance conditions. There is, however, one important exception in the case of IOPO where resonant and well-detuned SH offers an additional advantage: if one desires appreciable quantum noise reduction at low frequencies (around zero), we find above that a strong feedback of the SH results in an improvement from 1/3 (zero SH detuning) to 2/3 of quantum noise reduction (large SH detuning parameter).

Perfect squeezing is found in the subharmonics  $\omega_{\pm}$  positioned at the multiples of the free spectrum range (FSR) from the degenerate frequency  $\omega$  for zero SH detuning when the OPO is driven close to the threshold and the intracavity losses are negligible compared to the coupler transmission. The physical origin of this effect is, of course, in quantum correlations between the fields with frequencies obeying  $\omega_+ + \omega_- = 2\omega$ . For zero SH detuning our noise spectra reduce to Lorentzians with a width of  $2(\kappa + \gamma)$  centered at the multiples of the FSR frequency. For nonzero detunings we find that squeezing in the optimized quadrature degrades as a result of dephasing of the second harmonic.

From a practical perspective, the most attractive result of this squeezing at subharmonic frequencies (shown in Fig. 5) is that the amplitude quantum noise of light reflected off the nonlinear cavity can be completely suppressed around the FSR frequency and its multiples under ideal conditions. The ideal conditions include also perfect mode matching of the pump to the cavity. This result is valid regardless of the SH finesse of the resonator within our plane-wave approximation and the SH adiabatic approximation.

Since the FSR frequency is normally in the hundreds of MHz range, technical noise of the fundamental field can be very low there, so that the IOPO becomes an alternative to the broadband squeezed light sources. The signal to be detected with sub-shot-noise sensitivity should in this case be encoded at the FSR frequency. Such a system may prove to be a less complicated squeezer where an experimentalist has to deal with 'just' mode matching and tuning of one cavity.

*Acknowledgements.* This work has been supported by the Danish Natural Science Research Council.

## References

1. H.J. Kimble: Quantum Fluctuations in Quantum Optics – Squeezing and Related Phenomena. Lecture notes, Les Houches LIII (1990), ed. by J. Dalibard, J.M. Raimond, J. Zinn-Justin
2. For a recent update see: Quantum Semiclass. Opt. **9**(2) (1997). Special issue on  $\chi^{(2)}$  Nonlinear Optics, ed. by C. Fabre, J.P. Pochole. Or

- look in Opt. Express **2**(3) (1998).  
Found at <http://epubs.osa.org/opticsexpress/>
3. K. Bencheikh, C. Simonneau, J.A. Levenson: Phys. Rev. Lett. **78**, 34 (1997)
4. R. Bruckmeier, K. Schneider, S. Schiller, J. Mlynek: Phys. Rev. Lett. **78**, 1243 (1997)
5. M. Xiao, L.A. Wu, H.J. Kimble: Phys. Rev. Lett. **59**, 278 (1987).
6. P. Grangier, R.E. Slusher, B. Yurke, A. LaPorta: Phys. Rev. Lett. **59**, 2153 (1987)
7. E.S. Polzik, J. Carri, H.J. Kimble: Phys. Rev. Lett. **68**, 3020 (1992)
8. N.Ph. Georgiades, E.S. Polzik, K. Edamatsu, H.J. Kimble, A.S. Parkins: Phys. Rev. Lett. **75**, 3426 (1995)
9. J.L. Sørensen, J. Hald, E.S. Polzik: Phys. Rev. Lett. **80**, 3487 (1998)
10. J.L. Sørensen, J. Hald, N. Jørgensen, J. Erland, E.S. Polzik: Quantum Semiclass. Opt. **9**, 239 (1997)
11. E.S. Polzik, J. Carri, H.J. Kimble: Appl. Phys. B **55**, 279 (1992)
12. K. Schneider, M. Lang, J. Mlynek, S. Schiller: Opt. Express **2**, 59 (1998). Found at <http://epubs.osa.org/opticsexpress/>
13. M.A.M. Marte: Phys. Rev. Lett. **74**, 4815 (1995)
14. M.A.M. Marte: Phys. Rev. A **49**, R3166 (1994)
15. M.A.M. Marte: J. Opt. Soc. Am. B **12**, 2296 (1995)
16. S. Schiller, R.L. Byer: J. Opt. Soc. Am. B **10**, 1696 (1993)
17. S. Schiller, G. Breitenbach, R. Paschotta, J. Mlynek: Appl. Phys. Lett. **68**, 3374 (1996)
18. S. Schiller, R. Bruckmeier, A.G. White: Opt. Comm. **138**, 158 (1997)
19. S.F. Pereira, M. Xiao, H.J. Kimble, J.L. Hall: Phys. Rev. A **38**, R4931 (1988)
20. A. Sizmann, R.J. Horowicz, G. Wagner, G. Leuchs: Opt. Comm. **80**, 138 (1990)
21. R. Paschotta, M. Collett, P. Kurz, K. Fiedler, H.A. Bachor, J. Mlynek: Phys. Rev. Lett. **72**, 3807 (1994)
22. H. Tsuchida: Opt. Lett. **20**, 2240 (1995)
23. T.C. Ralph, M.S. Taubman, A.G. White, D.E. McClelland, H.A. Bachor: Opt. Lett. **20**, 1316 (1995)
24. A.G. White, P.K. Lam, M.S. Taubman, M.A.M. Marte, S. Schiller, D.E. McClelland, H.A. Bachor: Phys. Rev. A **55**, 4511 (1997)
25. M.J. Collett, R.B. Levien: Phys. Rev. A **43**, 5068 (1991)
26. P. Lodahl, Master thesis, Aarhus University (1997)
27. M.D. Reid, P.D. Drummond: Phys. Rev. A **40**, 4493 (1989)
28. P.D. Drummond, M.D. Reid: Phys. Rev. A **41**, 3930 (1990)
29. S. Reynaud, C. Fabre, E. Giacobino: J. Opt. Soc. Am. B **4**, 1521 (1987)
30. S. Reynaud, A. Heidmann: Opt. Comm. **71**, 209 (1989)
31. S. Chaturvedi, P.D. Drummond: Phys. Rev. A **55**, 912 (1997)
32. S.M. Barnett, P.L. Knight: J. Opt. Soc. Am. B **2**, 467 (1985)
33. C.J. Mertens, T.A.B. Kennedy, S. Swain: Phys. Rev. Lett. **71**, 2014 (1993)
34. J. Maeda, K. Kikuchi: Opt. Lett. **21**, 821 (1996)
35. M.J. Collett, D.F. Walls: Phys. Rev. A **32**, 2887 (1985)